Broadband Single- and Double-Balanced Resistive HEMT Monolithic Mixers

T. H. Chen, *Member, IEEE,* K. W. Chang, S. B. T. Bui,
L. C. T. Liu, *Member, IEEE,* G. S. Dow, *Member, IEEE,* and S. Pak

Abstract— **A double-balanced (DB) 3–18 GHz and a single-balanced (SB) 2–16 GHz resistive HEMT monolithic mixer have been successfully developed. The DB mixer consists of a AlGaAs/InGaAs HEMT quad, an active LO balun, and two passive baluns for RF and IF. At 16 dBm LO power, this mixer achieves the conversion losses of 7.5–9 dB for 4–13 GHz RF and 7.5–11 dB for 3–18 GHz RF. The SB mixer consists of a pair of AlGaAs/InGaAs HEMT's, an active LO balun, a passive IF balun and a passive RF power divider. At 16 dBm LO power, this mixer achieves the conversion losses of 8–10 dB for 4–15 GHz RF and 8–11 dB for 2–16 GHz RF. The simulated conversion losses of both mixers are very much in agreement with the measured results. Also, the DB mixer achieves a third-order input intercept (IP_3) of +19.5 to +27.5 dBm for a 7–18 GHz RF and 1 GHz IF at a LO drive of 16 dBm while the SB mixer achieves an input IP_3 of +20 to +28.5 dBm for 2 to 16 GHz RF and 1 GHz IF at a 16 dBm LO power. The bandwidth of the RF and LO frequencies are approximately 6:1 for the DB mixer and 8:1 for the SB mixer. The DB mixer of this work is believed to be the first reported DB resistive HEMT MMIC mixer covering such a broad bandwidth.**

I. Introduction

At THE PRESENT time, Schottky diode mixers are the most commonly used mixers in microwave systems. However, they have relatively poor intermodulation and spurious response properties due to their strongly nonlinear characteristics. Although various circuit schemes have been proposed to improve the intermodulation performance of the diode mixers [1]–[4], they either are not practical for wide frequency band application or require a massive LO power. Three-terminal devices, such as MESFET's and HEMT's, when used as mixing elements can achieve better performance and require less LO power than diode mixers [5]–[7]. Both MESFET's and HEMT's can be used as mixing elements in either an active or a resistive mode. The resistive mixer has the advantages of low noise figure, high two-tone third-order intermodulation intercept point, and low dc power consumption when compared with a corresponding active mixer [8]. In addition, a resistive HEMT mixer requires lower LO power and can operate over a wider frequency range than a resistive MESFET mixer because it has a steeper variation characteristic for the channel resistance between the off and on states and a smaller rc product value of the on-resistance and gate capacitance. This paper describes a single-balanced resistive HEMT mixer which downconverts a 2 to 16 GHz RF to a 0.75 to 1.25 GHz IF and a double-balanced resistive HEMT mixer which downconverts a 3 to 18 GHz RF to a 0.75 to 1.25 GHz IF.

Manuscript received January 20, 1993; revised June 6, 1994.

T. H. Chen was with TRW/ESG, ETD, M5/1065, Redondo Beach. CA 90278 USA. He is now with Hexawave Photonic Systems, Inc., Hsin Chu, Taiwan, ROC.

K. W. Chang, S. B. T. Bui, L. C. T. Liu, G. S. Dow, and S. Pak are with TRW/ESG, ETD, M5/1065, Redondo Beach, CA 90278 USA.

IEEE Log Number 9407458.

II. Device Modeling

In a HEMT amplifier, the HEMT operates in its saturation region and is used to transform the signal voltage applied to the gate into the drain current. The drain current, or the drain voltage if a load impedance were present at the drain, is varied by changing the gate voltage. However, in a resistive (passive) HEMT mixer, the HEMT operates in its ohmic (linear) region and is used as a variable resistor. The unbiased channel resistance is varied by changing the gate voltage. Ideally, the HEMT is treated as a switch controlled by the LO signal applied to the gate. The RF signal is then sampled at a rate determined by the LO frequency to achieve the frequency conversion.

Fig. 1 shows the nonlinear equivalent circuit of the HEMT device. Because of the large voltage swing of the LO signal applied to the gate, the gate-to-source and gate-to-drain characteristics are modeled by two diodes, allowing the effects of the gate current and the nonlinear gate capacitances to be taken into account. The gate diode models are constructed from the measured s-parameters and gate current-voltage characteristics. The drain-to-source current is modeled by a voltage-controlled current source. Most nonlinear device models available in commercial nonlinear simulators are mainly designed for active-mode operation [10]–[12] and cannot accurately describe the device behavior in the linear region where the resistive HEMT mixer operates. To overcome this problem, an user-defined model is developed and implemented in Libra of EEsof for this application. Fig. 2 shows the user-defined model of the voltage-controlled current source, I_{ds}. The current source's parameters are extracted by curve-fitting to measured I–V curves as shown in Fig. 3. This model accurately describes device characteristics in both linear and saturation regions. Other circuit element values are determined by curve-fittting to measured s-parameters of the HEMT device.

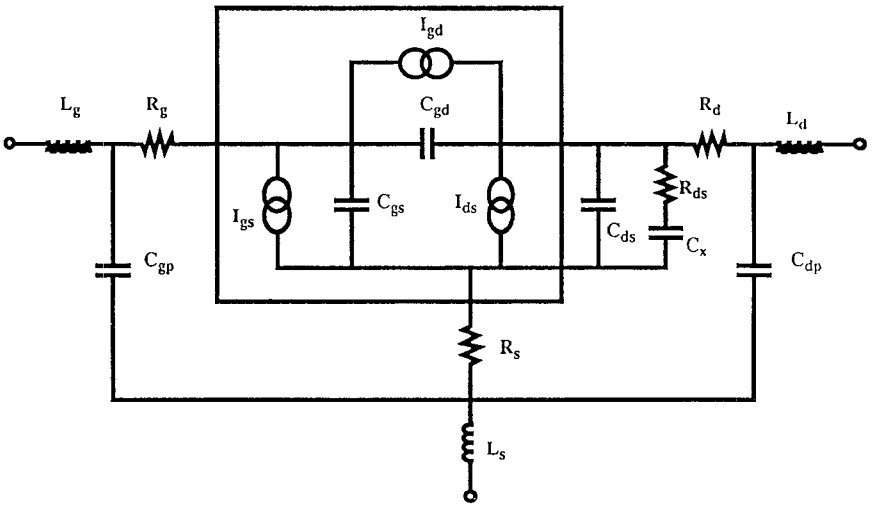

Fig. 1. Nonlinear equivalent circuit of the HEMT device.

$$I_{ds} = I_{dss}\tanh\left(d_1 V_{ds} + d_2 V_{ds}^2 + d_3 V_{ds}^3\right)$$

$$d_1 = 10^{\left[x_0 + x_1 V_{gs} + x_2 V_{gs}^2 + x_3 V_{gs}^3 + x_4 V_{gs}^4\right]} - 1$$

$$d_2 = 1 - 10^{\left[y_0 + y_1 V_{gs} + y_2 V_{gs}^2 + y_3 V_{gs}^3 + y_4 V_{gs}^4\right]}$$

$$d_3 = 10^{\left[z_0 + z_1 V_{gs} + z_2 V_{gs}^2 + z_3 V_{gs}^3 + z_4 V_{gs}^4\right]} - 1$$

$$I_{dss} = 10^{\left[g_0 - \exp\left(g_1 + g_2 V_{gs} + g_3 V_{gs}^2\right)\right]}$$

$$g_i = a_i + c_i\left(V_{dso} - V_{ds}\right) \qquad i = 0, 1, 2, 3, 4$$

Fig. 2. User-defined model.

III. Balanced Mixer Design

For a mixer to achieve broadband operation, the frequency ranges of one or more pairs of its signals (RF, LO, and IF) often overlap each other. Under the circumstances, a double-balanced (DB) or single-balanced (SB) mixer topology is required to provide isolation between the pair of signals having overlapped frequencies and spurious rejection over wide frequency range [9]. Although the DB mixer configuration outperforms the SB one in terms of port-to-port isolation and undesired signal rejection, the SB mixer configuration can operate over wider frequency band than its DB counterpart. This is because one of the bandwidth limiting baluns in a DB mixer is replaced by a power divider, which generally has wider bandwidth than a balun, in a SB mixer. Consequently, both mixer configurations are used in the broadband monolithic mixer designs.

Fig. 4(a) shows the circuit schematic of the double-balanced mixer. The mixer circuit consists of an AlGaAs/InGaAs HEMT quad, an active LO balun and two passive baluns, RF and IF. Four 160-μm AlGaAs/InGaAs HEMT's with 0.25-μm gate length are connected in a ring as the mixing devices. The HEMT acts as an variable resistor whose value is modulated by the LO signal voltage applied to the gate. The frequency conversion is achieved when a pair of balanced LO signals are used to switch ON and OFF in turn between two pairs of HEMT's of the quad while another pair of balanced RF signals are applied to two opposite nodes among the four of the quad. At the same time, two 180° out of phase IF signals appear at another two opposite nodes and are combined by the IF balun. Fig. 4(b) shows the circuit schematic of the single-balanced mixer. The mixer circuit consists of a pair of 320-μm AlGaAs/InGaAs HEMT's, an active LO balun, a passive IF balun and a passive RF power divider. Its principle of operation is similar to DB mixer's except that only two devices are used here and the IF signals appear at the same nodes as the ones RF signals are applied to.

Due to its capability of insertion gain and very broad bandwidth, an active LO balun is used for both DB and SB mixers. The active LO balun is composed of two four-section distributed amplifiers with one in common gate and the other in common source configuration. The total device periphery is 504 μm and the balun consumes about 100 mA current at 4-V drain voltage. To minimize the mixer's noise figure, passive baluns are used at the RF and IF ports for the DB mixer whereas a passive power divider and a passive balun are used at the RF and IF ports, respectively, for the SB mixer. The RF balun for the DB mixer is comprised of a two-section Wilkinson power divider and a pair of Lange couplers. One of the Lange couplers is loaded with the open circuits while the other is loaded with the short circuits. This balun can operate over a 4:1 bandwidth. For low IF frequencies, a compact lumped element balun is preferable to a distributed one for the IF port. In this design, a lumped-element ratrace hybrid is chosen for the IF balun due to its small size and up to 50% bandwidth. The IF balun is implemented with planar spiral inductors and MIM capacitors. For the SB mixer, the same two-section

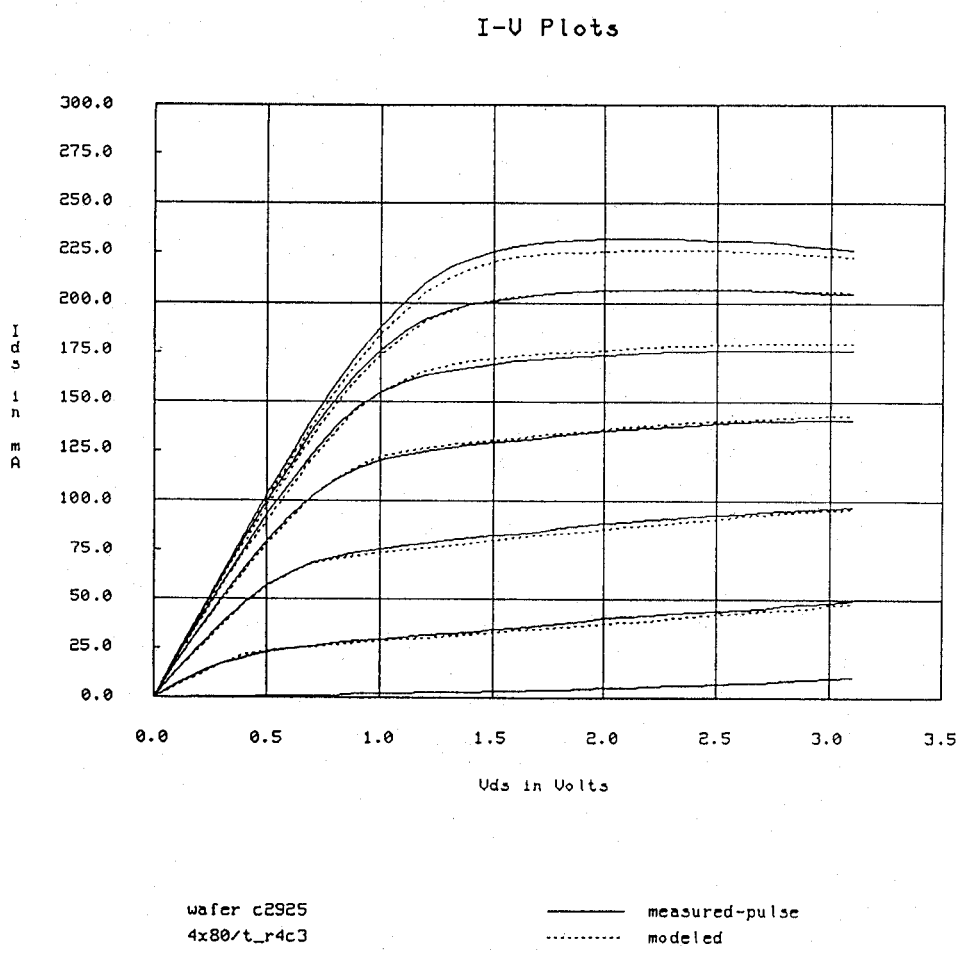

Fig. 3. Measured and modeled I–V curves of a 320-μm HEMT.

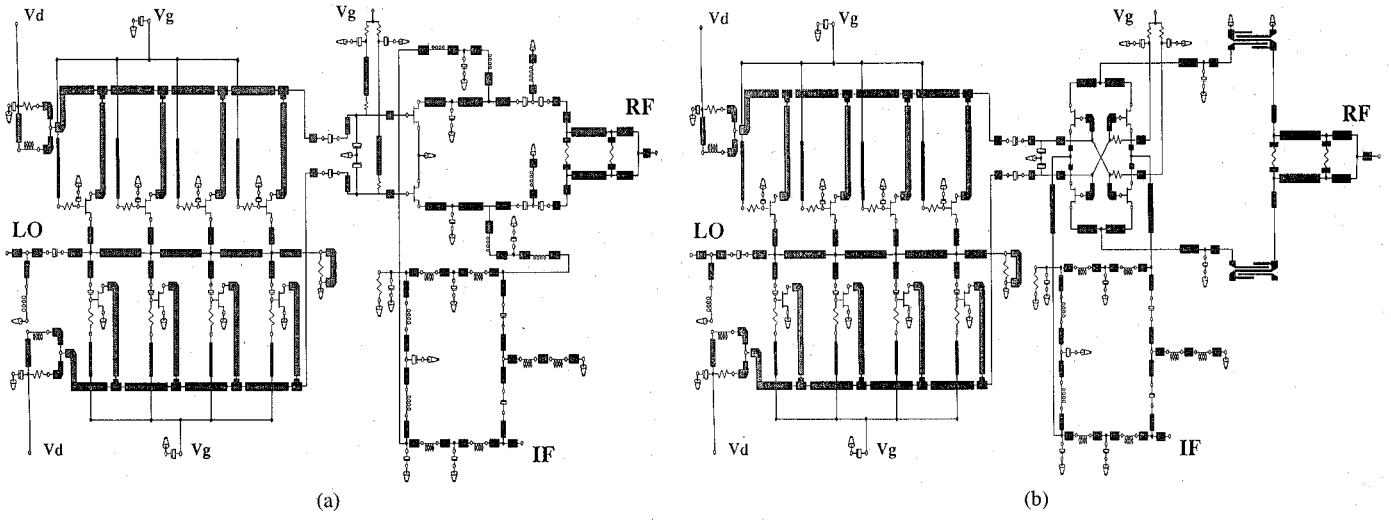

Fig. 4. (a) Circuit schematic of SB resistive HEMT mixer and (b) circuit schematic of DB resistive HEMT mixer.

Wilkinson power divider and IF balun as those in the DB mixer are used at the RF and IF ports, respectively. The power divider can achieve a nearly decade bandwidth. In addition, a pair of diplexers are used for the RF power divider and IF balun to separate the LO and RF signals from the IF signal. The diplexer consists of a high-pass and a low-pass filter implemented with planar spiral inductors and MIM capacitors.

The major degradation factors for the mixer using nonideal switches are the finite ON- and OFF-state resistances and finite

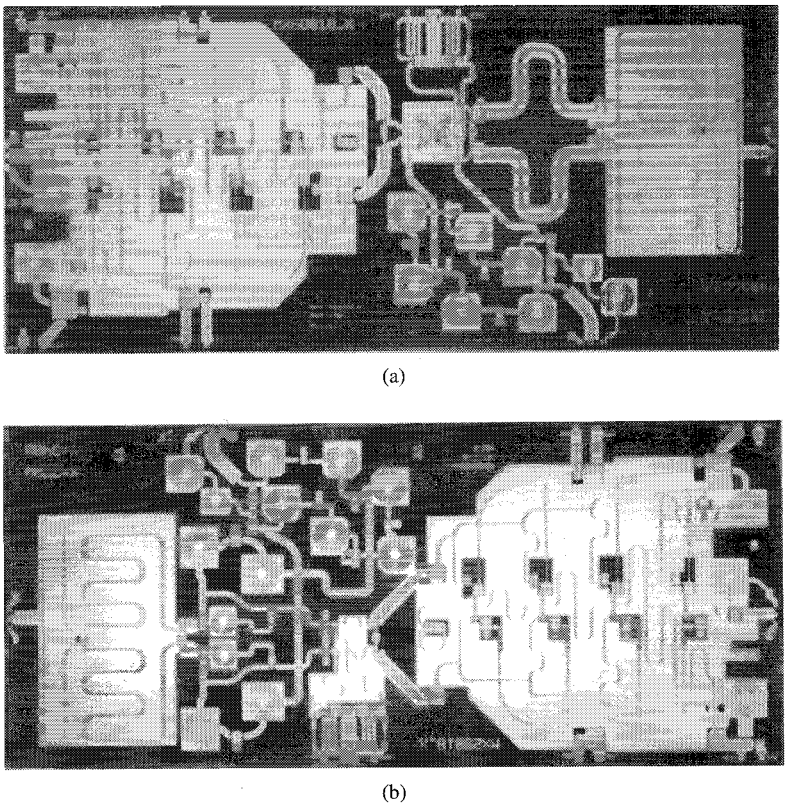

(a)

(b)

Fig. 5. (a) Photograph of SB resistive HEMT mixer chip (3.4 mm × 7.7 mm) and (b) photograph of DB resistive HEMT mixer chip (3.4 mm × 7.7 mm).

transition time between the ON and OFF states. Therefore, best performance of a resistive HEMT mixer is obtained when the devices are biased slightly below its pinch-off voltage and driven with a sufficient LO power to ensure hard and fast turn-on and turn-off. Other degradation factors, such as the gate-to-source, gate-to-drain and drain-to-source capacitances, the gate, drain and source series resistances, and parasitic inductances can be minimized by the matching techniques in most instances. In these two mixer designs, the HEMT devices used to mix RF and LO signals are biased at −1.3-V gate voltage while the HEMT devices inf the active LO balun are biased at −0.8-V gate voltage.

The mixer circuits were fabricated using a specially developed HEMT process [13] on an MBE-grown wafer with an AlGaAs/InGaAs heterostructure. Fig. 5 shows the photographs of the completed DB and SB monolithic mixer chips. Both mixer chips measure 3.4 × 7.7 mm^2.

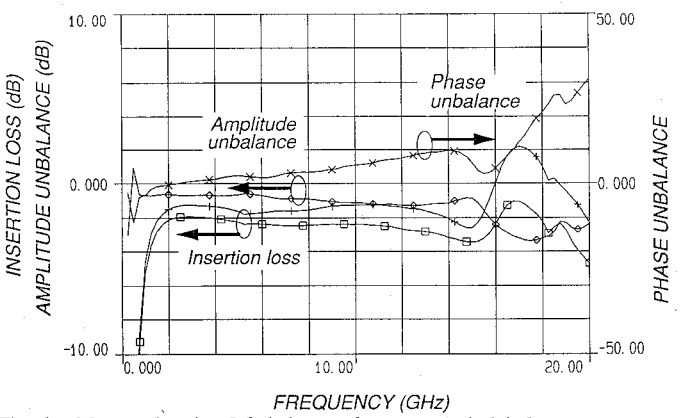

Fig. 6. Measured active LO balun performance (spiral inductors are constructed with landed metal lines).

IV. RF Performance

Three baluns, one power divider, one diplexer, and the monolithic DB and SB mixers were tested on-wafer with cascade RF probes. Fig. 6 shows the measured performance of an active LO balun. Over the 1.5–15.5 GHz frequency band, the amplitude and phase unbalances between the two balanced ports are less than 1.5 dB and 10°, respectively. Although, the simulated performance of the LO balun shows good amplitude and phase trackings between two balanced ports up to 20 GHz. The difference in performance above 15.5 GHz is believed to be caused by the self resonance of the 6-1/2-turns spiral inductor, which was not taken into account in the simulation. The measured insertion loss including the 3-dB power splitting loss is between 1.5 and 3 dB from 1.5–15.5 GHz. Fig. 7 shows the simulated performance of the RF power divider. The insertion loss including the 3-dB power splitting loss is between 3.5 and 4 dB from 1–20 GHz. Over the 2 to 20 GHz frequency band, the input and output return losses are better than 13 and 20 dB, respectively. Fig. 8 shows the measured performance of the RF balun. The insertion loss

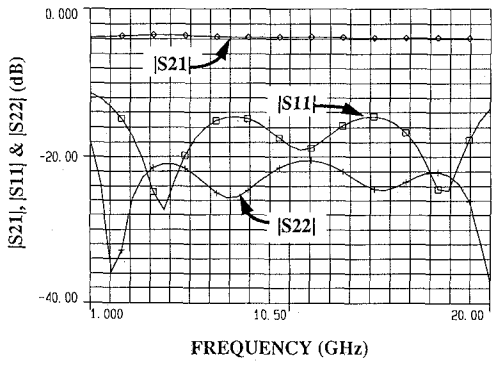

Fig. 7. Simulated passive power divider performance.

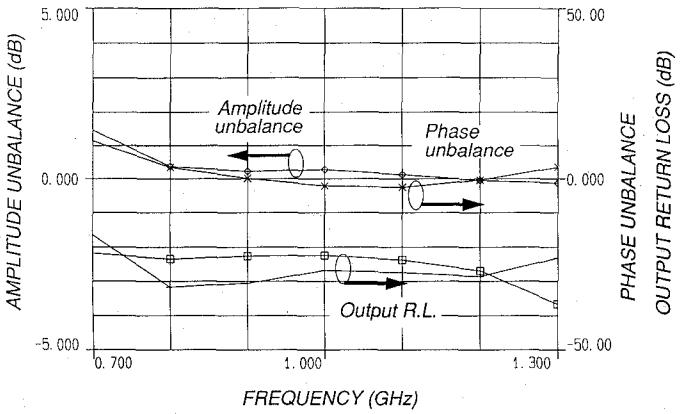

Fig. 9. Measured passive IF balun performance.

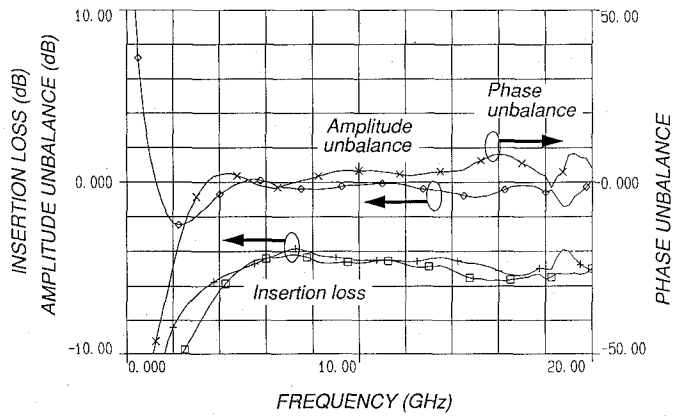

Fig. 8. Measured passive RF balun performance.

including the 3-dB power splitting loss is between 4 and 6 dB from 4–20 GHz. The amplitude and phase unbalances between two balanced ports are less than 1.5 dB and 8°, respectively, over the 4–20 GHz frequency band. The measured IF balun performance is in good agreement with the simulated result. Fig. 9 shows the measured amplitude and phase unbalances and return losses of the two balanced ports. The amplitude unbalance is less than 0.5 dB while the phase unbalance is less than 3° from 0.75–1.3 GHz. The return loss of the balanced ports is better than 22 dB for the same frequency band. The measured and simulated insertion losses and return losses of the diplexer are shown in Fig. 10 for the purpose of comparison. The agreement between them is very good for frequency up to 14.5 GHz. The differences above 14.5 GHz is also caused by the self resonance of the 6-1/2-turns spiral inductor, which was not taken into account in the simulation.

Fig. 11 shows the comparison between measured and simulated conversion losses of the DB HEMT resistive mixer as function of the RF frequency. A fixed IF frequency of 1 GHz and LO drive of 16 dBm were used. The measured conversion losses are between 7.5 and 9 dB for 4–13 GHz RF and 7.5 and 11 dB for 3–18 GHz RF. The agreement between the measured and simulated performances is within 1 dB from 2–14 GHz. The larger deviation between them at higher frequencies is due to the self resonance of the spiral inductor in the LO balun which was not taken into account in the simulation. Fig. 12 shows the comparison between measured and simulated conversion losses of the SB HEMT resistive mixer as a function of the RF frequency. A fixed IF frequency of 1 GHz and LO drive of 16 dBm were also used. The measured conversion losses are between 8 and 9 dB for 4–11 GHz RF and 8 and 11 dB for 2–16 GHz RF. The agreement between the measured and simulated is within 2 dB from 2–16 GHz. Again, the larger deviation between them at higher frequencies is due to the self resonance of the spiral inductors in the LO balun and diplexer. Fig. 13 compares three different measured conversion losses of the SB mixer to illustrate the effect of the self resonance of the spiral inductor on the mixer performance. The high end of the frequency band of the SB mixer is increased from 13.5–16 GHz by reducing parasitic capacitances associated with spiral inductors. Spiral inductors constructed with metal lines deposited directly on the substrate surface (landed metal lines) were replaced by metal lines suspended in air, which were constructed with the airbridge process. For the mixer using spiral inductors with airbridged lines, the conversion losses of both upper and lower sidebands are shown in Fig. 13, while for the mixer using spiral inductors with metal lines deposited on the substrate, only the upper sideband conversion loss is shown. In addition, the third-order input intercept (IP_3) of the DB and SB mixers are determined from an on-wafer two-tone intermodulation distortion measurement. A fixed 1-GHz IF and 16-dBm LO power were used. Figs. 14 and 15 show the measured input IP_3 of the DB mixer and SB mixer, respectively, as a function of the RF frequency. The input IP_3 of the DB mixer varies from 19.5–27.5 dBm for a RF of 7–18 GHz, while the input IP_3 of the SB mixer is between 20 and 28.5 dBm for a RF of 2–16 GHz.

Spurious rejections of the DB mixer were measured for a RF frequency between 10 and 11 GHz with an LO drive of 16 dBm and fixed IF frequency of 1 GHz. Fig. 16 summarizes the measured spurious rejections in a tabular form. Under the same operating condition, port-to-port isolations of the DB mixer were measured to be better than 30 dB from LO port to RF port, better than 38 dB from LO port to IF port, and

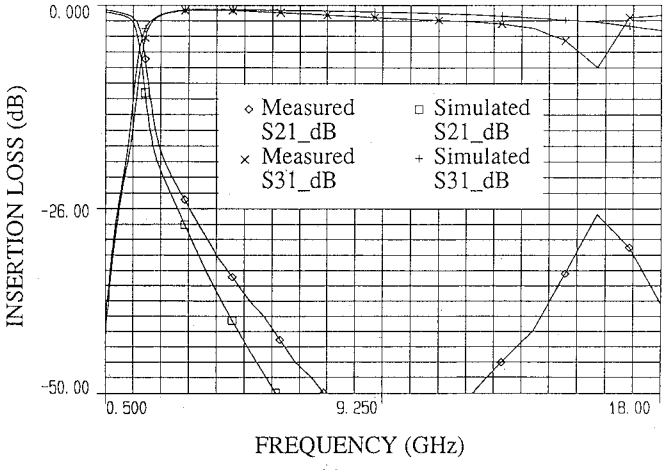

(a)

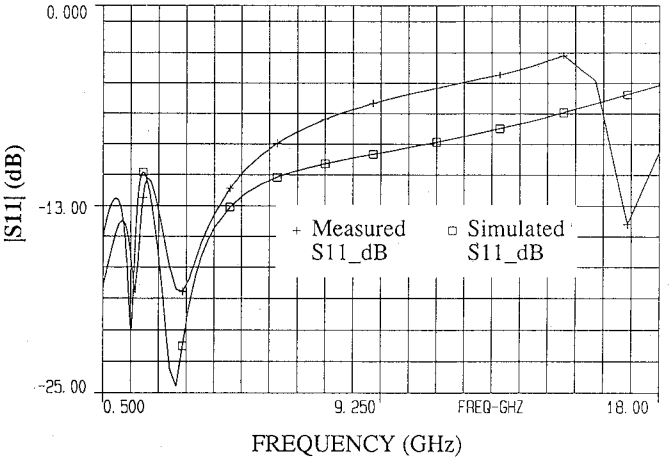

(b)

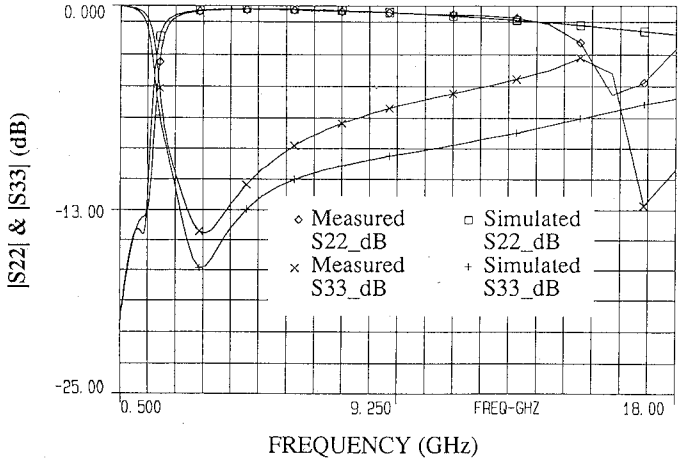

(c)

Fig. 10. Measured and simulated diplexer performance: (a) insertion loss, (b) input return loss, and (c) output return losses.

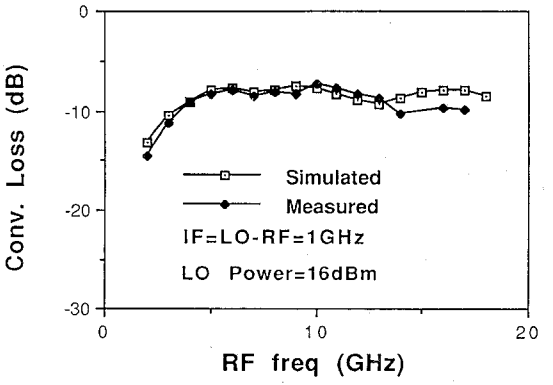

Fig. 11. Measured and simulated performance of DB resistive HEMT mixer (spiral inductors are constructed with airbridged metal lines).

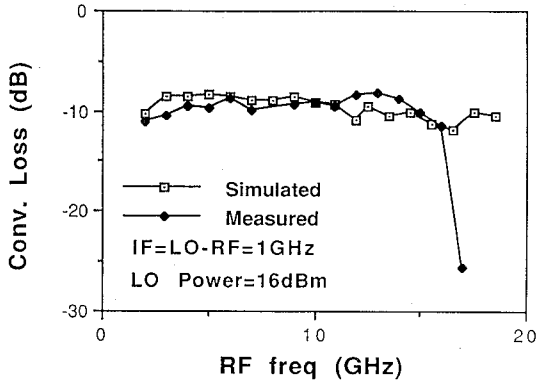

Fig. 12. Measured and simulated performance of SB resistive HEMT mixer (spiral inductors are constructed with airbridged metal lines).

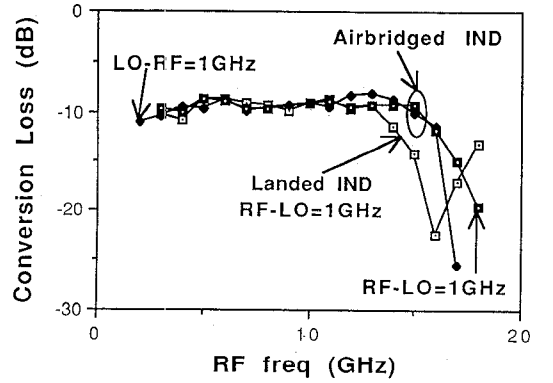

Fig. 13. Measured upper sideband conversion loss of SB mixer using spiral inductors with landed lines and measured upper and lower sideband conversion loss of SB mixer using spiral inductors with airbridged lines.

about 34 dB from RF port to IF port. Finally, temperature variations of the conversion loss and 2 × 3 as well as 3 × 2 spurious rejections of the DB mixers were also measured. The measured results are shown in Fig. 17 for the conversion loss and Fig. 18 for the spurious rejections. The variations of the conversion losses are less than 0.1 dB over the measured 15°C to 60°C temperature range for all mixers except the fifth one. These variations are within the measurement accuracy and consistent with what one can expect based on the theoretical prediction. The conversion loss of a resistive HEMT mixer is mainly determined by the LO power and the "on" state channel resistance of the HEMT devices at the maximum available LO

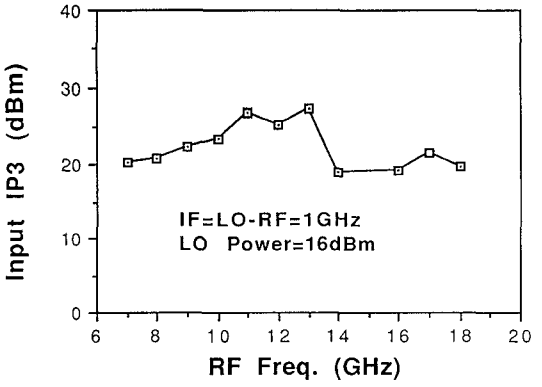

Fig. 14. Measured input IP_3 of DB resistive HEMT mixer as a function of the RF frequency.

Spur Rjection			
LO > RF		LO < RF	
RF × LO	Rejection,dBc	RF × LO	Rejection,dBc
2 × 1	47	1 × 2	20
2 × 2	46	2 × 1	51
3 × 1	61	2 × 2	60
3 × 2	68	2 × 3	63
3 × 3	59	2 × 4	65
4 × 2	80	3 × 2	>70
5 × 3	97	3 × 3	>70
6 × 4	100	3 × 4	>70

Fig. 16. Measured spurious rejections of the DB mixer.

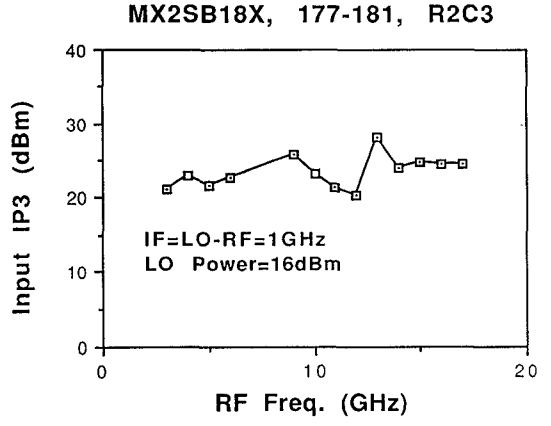

Fig. 15. Measured input IP_3 of SB resistive HEMT mixer as a function of the RF frequency.

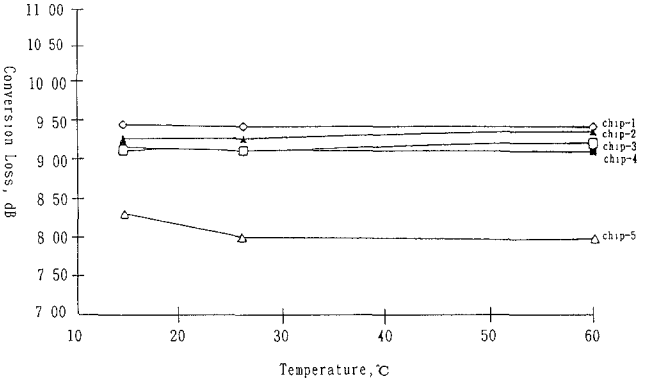

Fig. 17. Measured conversion loss as a function of the temperature for the DB mixers.

drive. In the saturation region of the conversion loss versus LO power curve, the conversion loss is only a weak function of the LO power and the "on" state channel resistance. The fifth mixer shows a 1/4-dB increase in conversion loss with decreased operating temperature and has the lowest conversion loss among five measured mixers. This may be due to the insertion gain of the active LO balun is higher so that the mixer is driven into deep saturation region. As a result, a further LO power increase due to lower operating temperature may degrade the mixer performance.

V. Conclusion

A multioctave SB-resistive HEMT monolithic mixer operating over a 2–16 GHz range and a multioctave DB-resistive HEMT monolithic mixer operating over a 3–18 GHz range have been successfully designed, fabricated, and tested. The SB mixer comprises a pair of AlGaAs/InGaAs HEMT's, an active LO balun, a passive RF power divider and a passive IF balun. The DB mixer consists of an AlGaAs/InGaAs HEMT quad, an active LO balun, and two passive baluns for RF and IF. The SB mixer chip has demonstrated a conversion loss of 8–10 dB for 4–15 GHz RF and a conversion loss of 8–11 dB for 2–16 GHz RF. As to the DB mixer chip, it has demonstrated a conversion loss of 7.5–9 dB for 4–13 GHz RF and a conversion loss of 7.5–11 dB for 3–18 GHz RF. The simulated conversion losses of both mixers are very much in agreement with the measured results. Furthermore, the DB mixer achieves a third-order input intercept of 19.5–27.5 dBm for 7–18 GHz RF and the SB mixer achieves an input IP_3 of 20–28.5 dBm for 2–16 GHz RF. Finally, the major bandwidth limiting factor, the self resonance of the 6-1/2-turns spiral inductor, of the original designs have been eliminated by using inductors constructed with air-bridged metal lines instead of metal lines deposited directly on the substrate. According to the measured data, the high end of the frequency band has been increased by about 12% for the DB mixer and 18% for the SB mixer, respectively.

Acknowledgment

The authors would like to thank Dr. D. Streit for the material growth, Dr. P. H. Liu, A. K. Oki, Dr. T. S. Lin, and E. Nattews for their help in the circuit fabrication, J. Coakley for his layout support and J. Roth, A. Lawerence IV, Prof. S. Mass, M. Tan, Dr. L. Wiedersphan, D. Yang, and S. Chen for their helpful discussions.

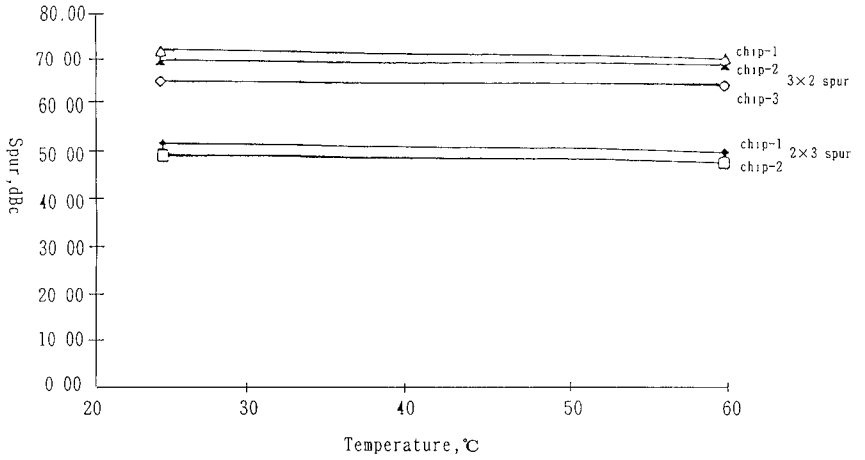

Fig. 18. Measured 2 × 3 and 3 × 2 spurious rejections versus temperature for the DB mixers.

REFERENCES

[1] E. F. Beane, "Prediction of mixer intermodulation levels as function of local oscillator power," *IEEE Trans. Electromagn. Compat.*, vol. EMC-13, pp. 56–63, May 1971.
[2] C. P. Tou and B. C. Chang, "A technique for intermodulation reduction in mixers," in *IEEE Symp. Electromagn. Compat. Dig.*, 1981, pp. 128–132.
[3] J. H. Lepoff and A. M. Cowley, "Improved intermodulation rejection in mixers," *IEEE Trans. Microwave Theory Tech.*, vol. MTT-14, pp. 618–623, Dec. 1966.
[4] J. Eisenberg *et al.*, "A new planar double-double-balanced MMIC mixer structure," in *IEEE 1991 Microwave and Millimeter-Wave Monolithic Circuit Symp. Dig.*, 1991, pp. 69–72.
[5] O. Kurita and K. Morita, "Microwave MESFET mixer," *IEEE Trans. Microwave Theory Tech.*, vol. MTT-24, pp. 361–366, June 1976.
[6] S. A. Maas, "Design and performance of a 45-GHz HEMT mixer," *IEEE Trans. Microwave Theory Tech.*, vol. MTT-34, pp. 799–803, 1986.
[7] S. Weiner *et al.*, "2 to 8 GHz double-balanced MESFET mixer with 30 dBm input 3rd order intercept," in *IEEE Microwave Theory Tech.-S Dig.*, 1988, pp. 1097–1100.
[8] S. A. Mass, "A GaAs MESFET mixer with very low intermodulation," *IEEE Trans. Microwave Theory Tech.*, vol. MTT-35, pp. 425–429, Apr. 1987.
[9] ——, *Microwave Mixers.* Norwood, MA: Artech House, 1986.
[10] W. R. Curtice and M. Ettenberg, "A nonlinear GaAs FET model for use in the design of output circuits for power amplifiers," *IEEE Trans. Microwave Theory Tech.*, vol. MTT-33, pp. 1383–1394, 1985.
[11] A. Materka and T. Kacprzak, "Computer calculation of large-signal GaAs FET amplifier characteristics," *IEEE Trans. Microwave Theory Tech.*, vol. MTT-33, pp. 129–135, Feb. 1985
[12] H. Statz *et al.*, "GaAs FET device and circuit simulation in SPICE," *IEEE Trans. Electron Dev.*, vol. ED-34, no. 2, pp. 160–169, Feb. 1987.
[13] T. H. Chen *et al.*, "A double-balanced 3-18 GHz Resistive HEMT Monolithic Mixer," in *IEEE 1992 Microwave and Millimeter-Wave Monolithic Circuit Symp. Dig.*, 1992, pp. 459–462.

T. H. Chen (M'93), photograph and biography not available at the time of publication.

K. W. Chang, photograph and biography not available at the time of publication.

S. B. T. Bui, photograph and biography not available at the time of publication.

L. C. T. Liu (S'77–M'81), photograph and biography not available at the time of publication.

G. S. Dow (S'78–M'82), photograph and biography not available at the time of publication.

S. Pak, photograph and biography not available at the time of publication.